



**HAL**  
open science

# Beyond the limits of the unassigned protist microbiome: inferring large-scale spatio-temporal patterns of marine parasites

Iris Rizos, Pavla Debeljak, Thomas Finet, Dylan Klein, Sakina-Dorothee  
Ayata, Fabrice Not, Lucie Bittner

## ► To cite this version:

Iris Rizos, Pavla Debeljak, Thomas Finet, Dylan Klein, Sakina-Dorothee Ayata, et al.. Beyond the limits of the unassigned protist microbiome: inferring large-scale spatio-temporal patterns of marine parasites. *ISME Communications*, 2023, 3 (16), 10.1101/2022.07.24.501282 . hal-03993694

**HAL Id: hal-03993694**

**<https://hal.science/hal-03993694>**

Submitted on 17 Feb 2023

**HAL** is a multi-disciplinary open access archive for the deposit and dissemination of scientific research documents, whether they are published or not. The documents may come from teaching and research institutions in France or abroad, or from public or private research centers.

L'archive ouverte pluridisciplinaire **HAL**, est destinée au dépôt et à la diffusion de documents scientifiques de niveau recherche, publiés ou non, émanant des établissements d'enseignement et de recherche français ou étrangers, des laboratoires publics ou privés.



Distributed under a Creative Commons Attribution - NonCommercial - NoDerivatives 4.0  
International License

1 **Beyond the limits of the unassigned protist**  
2 **microbiome: inferring large-scale spatio-temporal**  
3 **patterns of marine parasites**

4

5 Iris Rizos<sup>1,2</sup>, Pavla Debeljak<sup>1</sup>, Thomas Finet<sup>1</sup>, Dylan Klein<sup>1</sup>, Sakina-Dorothee Ayata<sup>3</sup>, Fabrice Not<sup>2</sup>,  
6 Lucie Bittner<sup>1,4</sup>

7

8 <sup>1</sup> Institut de Systématique, Evolution, Biodiversité (ISYEB), Muséum National d'Histoire Naturelle,  
9 CNRS, Sorbonne Université, EPHE, Université des Antilles, Paris, France, iris.rizos@sb-roscoff.fr

10 <sup>2</sup> Sorbonne Université, CNRS, AD2M-UMR7144 Station Biologique de Roscoff, 29680 Roscoff,  
11 France

12 <sup>3</sup> Sorbonne Université, Laboratoire d'Océanographie et du Climat : Expérimentation et Analyses  
13 Numériques (LOCEAN, SU/CNRS/IRD/MNHN), 75252 Paris Cedex 05, France

14 <sup>4</sup> Institut Universitaire de France, Paris, France

15

16 The authors declare that they have no conflict of interest.

17

18

19

20

21

22

23

24

25 **Abstract**

26 Marine protists are major components of the oceanic microbiome that remain largely unrepresented

27 in culture collections and genomic reference databases. The exploration of this uncharted protist  
28 diversity in oceanic communities relies essentially on studying genetic markers from the environment  
29 as taxonomic barcodes. Here we report that across 6 large scale spatio-temporal planktonic surveys,  
30 half of the genetic barcodes remain taxonomically unassigned at the genus level, preventing a fine  
31 ecological understanding for numerous protist lineages. Among them, parasitic Syndiniales  
32 (Dinoflagellata) appear as the least described protist group. We have developed a computational  
33 workflow, integrating diverse 18S rDNA gene metabarcoding datasets, in order to infer large-scale  
34 ecological patterns at 100% similarity of the genetic marker, overcoming the limitation of taxonomic  
35 assignment. From a spatial perspective, we identified 2 171 unassigned clusters exclusively shared  
36 between the Tropical/Subtropical Ocean and the Mediterranean Sea among all Syndiniales orders  
37 and 25 ubiquitous clusters shared within all the studied marine regions. From a temporal perspective,  
38 over 3 time-series, we highlighted 38 unassigned clusters that follow rhythmic patterns of recurrence  
39 and are the best indicators of parasite community's variation. These clusters withhold potential as  
40 ecosystem change indicators, mirroring their associated host community responses. Our results  
41 underline the importance of Syndiniales in structuring planktonic communities through space and  
42 time, raising questions regarding host-parasite association specificity and the trophic mode of  
43 persistent Syndiniales, while providing an innovative framework for prioritizing unassigned protist  
44 taxa for further description.

45

## 46 **Introduction**

47 The advances in high-throughput sequencing technologies have provided a new perspective to  
48 microbial diversity at a global scale. Studying the DNA of environmental microbial communities (i.e.  
49 microbiome) allowed to overcome the limit of non-cultivability and provided access to an  
50 unprecedented large quantity of high resolution genetic information [1-4]. *In silico* downstream  
51 analysis of genetic big-data shed light on a new challenge in microbial ecology: exploring the  
52 unassigned microbiome [5,6]. From the point of view of environmental genomics, the unassigned  
53 microbiome encompasses all genetic sequences that cannot be annotated with referenced biological  
54 information as they have no match in databases at a functional [6-9] and/or taxonomic level [5, 10,  
55 11]. Recent studies have pointed out that unassigned sequences contribute to 25-58% of microbial

56 communities' diversity observed across a variety of aquatic and soil ecosystems [4, 5, 12]. In the  
57 marine realm, large scale sequencing studies have revealed that the unassigned microbiome  
58 represents half of the functional diversity (including samples enriched in viruses, prokaryotes and  
59 protists) [13]. In terms of taxonomic diversity, the unassigned protist microbiome, defined as taxa  
60 with V9 regions of the 18S rDNA marker having a sequence similarity <80% with reference  
61 sequences, represents ~30% at the supergroup level ([14].

62

63 In marine metabarcoding studies, Syndiniales (a clade of marine alveolates, MALVs [15]) represent  
64 an ubiquitous and hyperdiverse lineage of protistan endoparasites [16-18]. Syndiniales are  
65 distributed worldwide from tropical and temperate zones [14, 19] to both arctic and antarctic poles  
66 [20, 21]. Their unexpected contribution to protist community composition has been revealed by  
67 metabarcoding studies both in open sea and coastal environments, with Syndiniales being the third  
68 most abundant lineage of the circumglobal Tara Oceans expedition [14] and representing up to 11%  
69 of community's abundance in fjordic-bays [21] and 28% at a North-Atlantic river estuary [22].  
70 Accumulating observations and correlations of metabarcoding data support that Syndiniales are  
71 opportunistically infecting a wide spectrum of hosts, including other protists (dinoflagellates, ciliates,  
72 radiolarians) but also metazoans (e.g. crustaceans) [22-23]. Their wide abundance and distribution  
73 confers them global ecological importance for microbial food webs and biogeochemical cycling, by  
74 regulating host populations [22, 24, 25] and supplying the microbial loop with organic matter [26].  
75 Yet, the great majority of Syndiniales remain uncultivable and show a high degree of divergence in  
76 genomic sequences [27]. A recent study in an estuary revealed the existence of at least 8 cryptic  
77 Syndiniales species, among which 6 could be differentiated by the V4 region of the 18S marker by  
78 an 100% sequence similarity threshold [17]. Moreover, their complex lifestyle, small size (< 20 µm)  
79 and lack of distinctive morphological features makes Syndiniales' description a laborious process  
80 relying on designing specific probes for *in situ* hybridization [24, 25, 28]. Thus, Syndiniales diversity  
81 still remains a blackbox in protistology [22, 25, 29], rendering the ecological understanding of these  
82 widespread microorganisms below the order level presently beyond reach [17].

83

84 In this study, we explored marine planktonic protist communities at a wide spatio-temporal scale, in  
85 order to: (i) quantify the taxonomically unassigned sequences and reveal protist lineages for which  
86 there is a major scarcity of taxonomic references, (ii) highlight unassigned protist diversity shared  
87 between contrasted marine environments and (iii) identify unassigned taxa which are ecologically  
88 relevant and recurrent, that should be prioritized for further characterisation. We integrated 12 years  
89 of data and 155 different sampling locations from 6 environmental metabarcoding datasets,  
90 combining 3 coastal time-series (ASTAN, BBMO, SOLA), 1 European coastal Sea sampling project  
91 (BioMarKs) and 2 oceanographic campaigns (Malaspina, MOOSE). As a study case, we focused our  
92 analyses on the parasite group of Syndiniales and, by clustering the gathered metabarcodes in a  
93 Sequence Similarity Network (SSN), we revealed novel ecological patterns of Syndiniales at a  
94 taxonomic resolution of 100% similarity between V4 regions of the 18S rDNA marker.

## 95 **Results**

### 96 ***Diversity and abundance of taxonomically unassigned protists: the uncharted territory of*** 97 ***Syndiniales***

98 Among the 343 165 metabarcodes we considered in our study (Table S1), those that were  
99 taxonomically unassigned at a given taxonomic rank (i.e., without any match with reference  
100 sequences under 80% of sequence similarity) according to the PR2 or SILVA reference databases  
101 were considered as unassigned at this taxonomic rank (Fig. S1A). Unassigned metabarcodes  
102 occurred in every sampled region and at every taxonomic rank, from kingdom to species (Fig. 1A,  
103 Fig. S2). Both the relative abundance and number of unassigned metabarcodes increased from high  
104 to low taxonomic ranks contributing respectively to an average of 0.03% and 0.28% of the whole  
105 protist community at the kingdom rank and to 69.35% and 82.67% at the species rank (Fig. 1A, Fig.  
106 S3B). At kingdom level, 628 metabarcodes remained unassigned among which 87.70% originated  
107 from bathypelagic samples (2 150 - 4 000 m) of the Malaspina expedition (Fig. S4). The biggest  
108 increase in unassigned metabarcode proportion was observed from family to genus level for which  
109 71.14% and 58.95% of metabarcodes were unassigned in relative number and relative abundance  
110 respectively (increase of 35% in unassigned metabarcodes). Overall, at the lowest taxonomic levels

111 of our global dataset, i.e. genus and species, the proportion of unassigned metabarcodes was similar  
112 and represented more than half of the metabarcodes that could not be assigned to any referenced  
113 protist taxon (Fig. 1A). The study of unassigned sequences was thus conducted from the viewpoint  
114 of the genus taxonomic level.

115

116 Across protist divisions, a higher diversity index was obtained for unassigned metabarcodes  
117 belonging to Dinoflagellata for all datasets (Fig. 1B). Overall, 54% of unassigned metabarcodes in  
118 relative number and 63% in relative abundance belonged to Dinoflagellata (Fig. S4A). Among other  
119 protist divisions lacking taxonomic assignment at the genus level were Ochrophyta (all datasets),  
120 Ciliophora (BioMarKs, SOLA, Malaspina, MOOSE), Radiolaria (BioMarKs, Malaspina, MOOSE),  
121 Cercozoa (ASTAN, SOLA), Cryptophyta (BioMarKs, ASTAN, BBMO), Opalozoa (ASTAN, BBMO,  
122 SOLA, MOOSE) and Sagenista (BioMarKs, BBMO, Malaspina) (Fig. S5A). A higher diversity index  
123 was obtained for unassigned sequences, compared to assigned sequences, for the divisions  
124 Opalozoa, Sagenista and Cercozoa (Fig. S5B). Thus, when studying only assigned genera of the  
125 latter protist divisions, their diversity could be largely underestimated.

126

127 Dinoflagellata metabarcodes represent 52% of our global dataset (179 615 metabarcodes). Among  
128 unassigned Dinoflagellata, Dinophyceae and Syndiniales were the two dominant classes and  
129 Syndiniales represented 66% and 48% of metabarcodes in terms of number and abundance  
130 respectively (Fig. S6A). Within these two classes, the proportion of unassigned metabarcodes at the  
131 genus level was 2-fold higher for Syndiniales, with 98% and 95% of metabarcodes unassigned in  
132 terms of relative number and abundance (Fig. 1C, Fig. S6B). Only 4 species of Syndiniales had a  
133 taxonomic assignment (0.01% of total metabarcodes and 0.53% of Syndiniales metabarcodes).  
134 Syndiniales metabarcodes unassigned at genus level represented 21% of our global dataset (72 789  
135 metabarcodes). Given the contribution and overwhelming majority of unassigned Syndiniales in our  
136 dataset, we decided to focus the rest of our study on this lineage.

137

138 ***Shared patterns of unassigned Syndiniales diversity between sunlit Mediterranean and***

### 139 ***Tropical waters***

140 To investigate the spatio-temporal distribution of Syndiniales at genus level we built connected  
141 components (CCs), i.e clusters of metabarcodes with 100% sequence identity and a minimum of 80%  
142 coverage. We consider the CCs as a proxy for clustering metabarcodes of the same Syndiniales  
143 genera or at least as pragmatic units to deal with Syndiniales molecular diversity across multiple  
144 datasets. After clustering, our global dataset contained 4 317 Syndiniales CCs (30% of all CCs) out  
145 of which 4 245 CCs were unassigned at the genus level (98% of Syndiniales CCs) (Fig. S7A). These  
146 unassigned CCs belonged to 5 orders of Syndiniales, Dino-Group-I to III, Dino-Group-V and an  
147 “Unknown” order (rank not assigned). Out of the unassigned Syndiniales CCs, 58% (2 478 CCs)  
148 were exclusively shared within 2 sea regions, being mainly the Tropical/Subtropical Ocean and the  
149 Mediterranean Sea (which both include samples at depth > 1 000 m), regrouping 51% of the  
150 unassigned Syndiniales CCs (2 171 CCs) (Fig. 2, N=2). Unassigned CCs endemic to one region  
151 represented 23% of Syndiniales CCs (961 CCs) and were mostly found at the surface of the  
152 Tropical/Subtropical ocean (Fig. 2, N=1), while 12% of CCs (518 CCs) were shared between 3  
153 regions (Fig. 2, N=3) and 7% CCs (288 CCs) were shared between more than 3 regions (Fig. 2,  
154 N>3). All studied sea regions shared 25 ubiquitous unassigned Syndiniales CCs, including 14 CCs  
155 belonging to the Dino-Group-II Syndiniales order (Fig. 2, N=6).

156

157 Among Syndiniales orders, Dino-Group-II and Group-I were the most represented in our dataset (2  
158 954 CCs, 70%; 1 056 CCs, 25% of unassigned Syndiniales CCs respectively (Fig. S7B)) and their  
159 distribution was mostly restricted to the Subtropical Ocean and Mediterranean Sea (Fig. 2). Dino-  
160 Group-III (212 CCs, 5% of unassigned Syndiniales CCs (Fig. S7B)) had the widest distribution,  
161 including diversity shared between many different pairs of regions with some patterns being unique  
162 to this order, i.e CCs that were exclusively common between the Bay of Biscay and the  
163 Mediterranean Sea and between the Black Sea and the Mediterranean Sea (Fig. 2, N=2). Dino-  
164 Group-V included 13 CCs (0.3% of unassigned Syndiniales CCs (Fig. S6)) and included CCs  
165 exclusively shared between the English Channel and the Tropical/Subtropical Ocean (Fig. 2, N=2).  
166 The Unknown Syndiniales order included 10 CCs (0.2% of unassigned Syndiniales CCs (Fig. S7B))

167 and was found in 3 sea regions: Mediterranean Sea, Tropical/Subtropical Ocean (main pattern for  
168 this order, 9 CCs) and North Sea (1 CC shared between the 3 mentioned sea regions) (Fig. 2).

169

170 Since for all Syndiniales orders 50% of unassigned CCs were found to be exclusively common to  
171 mediterranean and tropical regions we further explored how this pattern was distributed across the  
172 water column. Among the 2 171 CCs exclusively shared between mediterranean and tropical waters,  
173 Syndiniales communities were the most similar in the photic zone with 63% of CCs common between  
174 DCM (Deep Chlorophyll Maximum) layers and ~30% common between surface and DCM  
175 reciprocally (34% CCs common between Tropical/Subtropical Ocean DCM and Mediterranean Sea  
176 surface; 32% CCs common between mediterranean DCM and Tropical/Subtropical Ocean, n.b.  
177 percentages are indicative of major trends and not proportion as combinations are not exclusive)  
178 (Fig. 3A). Notably, a pattern of shared Syndiniales CCs was also found between bathypelagic  
179 samples from the Mediterranean Sea and samples from the photic zone of the Tropical/Subtropical  
180 Ocean (29% CCs) (Fig. 3A).

181

182 In order to test if these shared diversity patterns can be explained by similar physicochemical  
183 conditions, we explored the abundance variation of unassigned Syndiniales CCs in the  
184 mediterranean and tropical waters in an RDA using the physicochemical parameters as explanatory  
185 variables. The variation of physicochemical parameters explained ~10% (11.2% in first 6 RDA  
186 dimensions) of the abundance variation of unassigned Syndiniales CCs (Fig. 3B). Based on this  
187 result, two communities of Syndiniales could be distinguished according to the first two dimensions  
188 of the RDA: a deep water (> 200 m) community associated with colder and more eutrophic conditions  
189 (Fig. 3B, left) and a photic (surface and DCM) community associated with warmer and more  
190 oligotrophic conditions (Fig. 3B, right). In the RDA space associated with the photic zone,  
191 mediterranean and tropical samples partly overlap and correspond to warmer and less salty waters,  
192 hence providing an environmental basis for the observed Syndiniales pattern in these two marine  
193 environments (Fig. 3A).

194



195 To further investigate this hypothesis, we compared the community composition of protist divisions  
196 known to be major hosts for Syndiniales, between the marine regions of our global dataset. For  
197 Dinophyceae, Radiolaria and Ciliophora, the jaccard dissimilarity index was the lowest between  
198 Mediterranean sea and Tropical/Subtropical Ocean compared to community comparisons between  
199 the other sea regions (Table S2). This was also the case for Syndiniales, further supporting the  
200 results illustrated above (Fig. 3A). Neither of the remaining protist divisions found as having an  
201 important contribution to our dataset (Ochrophyta, Cercozoa, Cryptophyta, Opalozoa) showed the  
202 same tendency apart from Sagenista (Fig. S4, Table S2).

203

#### 204 ***Rhythmic ecological indicators among unassigned Syndiniales community***

205 Temporal aspects of the Syndiniales community were studied across the three time-series (ASTAN,  
206 BBMO, SOLA) in our dataset. Unassigned Syndiniales clusters did not indicate any clear seasonal  
207 preference based on monthly abundance for any of the time-series (Fig. S8). The correlation of CCs  
208 to the overall Syndiniales community dynamics and their rhythmicity was computed with two methods.  
209 The Escouffier's equivalent vectors selected the CCs that are the best indicators of community  
210 abundance variation according to a PCA and the Lomb-Scargle periodogram algorithm detected if  
211 CCs follow rhythmic patterns of occurrence across time. In the studied time-series, 75% of the  
212 Syndiniales community response to environmental variation was described by 45 CCs at ASTAN, 36  
213 CCs at BBMO and 17 CCs at SOLA (Table S3). These community indicator CCs were all unassigned  
214 at the genus level. Rhythmic occurrence among Syndiniales CCs was found to be more prevalent in  
215 the Western Channel with 208 rhythmic Syndiniales CCs found at ASTAN, 118 CCs found at BBMO  
216 and 15 CCs found at SOLA (Table S4). Some of the unassigned Syndiniales CCs were found to be  
217 both community indicators and rhythmic throughout the time-series: 27 CCs at ASTAN, 7 CCs at  
218 BBMO and 5 CCs at SOLA (Table S5). The average recurrence period of these clusters was ~1.5  
219 years at ASTAN and BBMO ~1 year at SOLA (Table S6). We identified two rhythmic indicator CCs  
220 shared between the time-series of the English Channel (i.e. ASTAN) and Mediterranean Sea (Fig.  
221 4): CC\_unknown\_154, shared with BBMO, and CC\_unknown\_183, shared with SOLA (recurrence  
222 periods are indicated in Table S6). One indicator CC, CC\_unknown\_126, was found to be shared

223 between all the studied time series (Fig. 4) with quicker recurrence periods in the Mediterranean  
224 (Table S6). All other rhythmic indicator CCs were specific to each time-series. CC\_unknown\_126  
225 was the CC with the highest monthly relative abundance at BBMO and SOLA, while having the 4th  
226 highest monthly relative abundance at ASTAN. The seasonal prevalence for the majority of rhythmic  
227 indicator CCs was up to 3 seasons (Fig. 4, Table S7). Rhythmic indicators with a 4 season prevalence  
228 occurred and were more numerous at the Western Channel. The shared indicator CC\_unknown\_126  
229 maintained a high seasonal prevalence occurring at 3 seasons in the Mediterranean Sea (i.e., BBMO  
230 and SOLA) and 4 seasons in the English Channel (i.e., ASTAN) (Fig. 4).

## 231 **Discussion**

### 232 ***What are we missing from eukaryotic diversity with metabarcoding ?***

233 In environmental genomics investigations, the 18S rDNA universal marker sequence constitutes the  
234 gold standard for the exploration of eukaryotic diversity in environmental communities, shedding light  
235 on uncultivable and rare taxa [16, 30]. Yet, by integrating different metabarcoding datasets, we report  
236 that in the marine realm half of protist sequences cannot be taxonomically assigned at the genus  
237 level (57% of sequences in our dataset) and these unassigned protist taxa represent 36% to 82% of  
238 the protist community in terms of abundance across 6 diverse marine environments. Few  
239 metabarcoding studies have quantified unassigned protist diversity. In Tara Oceans, unassigned  
240 protist diversity revealed with the V9 region of the 18S rDNA marker at the supergroup level was  
241 found to be <3% of total reads [14] when referring to unassigned sequences as marker sequences  
242 with <80% identity with reference sequences. Here, with the V4 region of the 18S rDNA marker we  
243 find that unassigned protist sequences represent in abundance <1% at the supergroup level. At the  
244 genus level unassigned sequences are not rare among the protist community as they represent in  
245 abundance >45% of metabarcodes in each studied dataset and up to 80% of metabarcodes for the  
246 Malaspina expedition dataset.

247

248 This confirms the current biased view of eukaryotic diversity, mostly focusing on multicellular and  
249 cultivable taxa, neglecting >70% of eukaryote diversity, including key lineages for the evolution of

250 life and to understand ecosystems functioning [30-32]. This missing picture can be addressed, for  
251 metabarcoding studies, in the context of sample acquisition but also data acquisition in reference  
252 databases. Some oceanic regions are more sampled than others, i.e. coastal locations compared to  
253 deep / open-sea environments [33]. Moreover, the maintenance and update of reference databases  
254 is a laborious but critical process whose pace is difficult to synchronize with the generation of an  
255 ever-increasing amount of environmental sequences [34]. Metabarcoding assessments of the  
256 diversity also depends on the choice of ribosomal marker genes. In our study, the largest proportion  
257 of unassigned protist diversity was found at low taxonomic levels, a trend that has also been  
258 observed for prokaryotes [6]. Universal ribosomal markers such as 16S rDNA and 18S rDNA can  
259 have a distinct taxonomic resolution depending on the lineage considered and within each lineage  
260 [30, 35], for instance in order to describe diatom diversity a threshold >95% similarity of the V9  
261 regions of the 18S rDNA gene with reference sequences delimits some genera (e.g. *Undatella*) while  
262 a threshold of <90% is sufficient for assigning some other genera (e.g. *Synedropsis*) [36].

263

#### 264 ***Perspectives on Syndiniales biogeography***

265 The challenge of barcoding marker taxonomic resolution is particularly relevant for rapidly evolving  
266 lineages, like predicted by evolutionary theory for parasites [37]. Studies on life history traits of  
267 multicellular parasites have demonstrated their quick adaptive plasticity, being involved in an  
268 evolutionary arms race with their host [37, 38]. Parasites are the most abundant component in many  
269 eukaryotic communities investigated through metabarcoding approaches, whether using high  
270 throughput sequencing technologies such as Illumina in tropical soils [40], subtropical marine  
271 ecosystems [39] and polar regions [20, 21], or low throughput cloning-sequencing methods in a  
272 lacustrine ecosystem [41]. In our study, parasitic Dinoflagellates (Syndiniales) represented 22% of  
273 metabarcodes and only 0.4% (1 537 metabarcodes) could be assigned to a referenced genus, being  
274 the major contributor to the unassigned marine protist microbiome. To capture efficiently Syndiniales  
275 diversity, an alternative would be to design specific primers as it has been done to target *Perkinsea*  
276 [42] and *Microsporidia* [43], or a combination of distinct genetic markers should be favored (e.g. 18S  
277 and ITS or COI) [43]. The cytochrome *c* oxidase 1 (COI) barcode has successfully identified different  
278 cultured dinoflagellate species [44]. Studies using the V9 and V4 regions of 18S rDNA marker [45]

279 to study the diversity of Dinoflagellata, retrieved different diversity patterns for each marker, stressing  
280 the difficulty to describe diverse, dominant lineages of protist communities.

281

282 When studying the distribution patterns of Syndiniales, we found CCs of the 100%-similar sequences  
283 shared between disconnected oceanic regions included along a latitudinal gradient from the North  
284 Sea to the South Subtropical Atlantic, Indian, and Pacific Oceans. Clarke *et al.*, 2019 have reported  
285 an OTU from Syndiniales Group I with identical V4 regions of the 18S rDNA marker to have been  
286 retrieved from surface samples in a Southern Ocean transect near sea-ice edge and seven different  
287 Northern Hemisphere coastal locations including tropical/subtropical zones. The putative inferred V9  
288 region of 18S rDNA marker of this abundant Syndiniales is present in every station of the Tara  
289 Oceans voyage, including mediterranean samples [20]. This suggests that closely related parasites  
290 can infect a wide range of hosts [20], which could also be the case for the shared Syndiniales CCs  
291 in our study. Our results indicated 50% (2 171 CCs) of the Syndiniales community in common  
292 between two tropical/subtropical waters and the mediterranean basin in the euphotic zone. In this  
293 case, a convergent selection of host-parasite systems in distant but physicochemically similar  
294 oligotrophic environments could also be hypothesized. Statistical analyses reported physicochemical  
295 similarities for surface waters of these marine environments and potential host communities showed  
296 greatest similarity in composition between the Tropical/Subtropical Ocean and the Mediterranean  
297 Sea. In that context, the shared Syndiniales CCs between bathypelagic tropical/subtropical and  
298 photic mediterranean layers could be linked to different life stages of hosts across the water column  
299 [46]. Complementary studies need to be done comparing open sea and coastal regions, using  
300 alternative markers to 18S rDNA to validate these observations. Further exploring host-parasite  
301 comparative biogeography patterns through co-occurrence networks could help elucidate the  
302 distribution extent of parasite associations at a global scale and allow to define more precisely host-  
303 ranges among parasites at low taxonomic resolution [47-49].

304

### 305 ***Perspectives on Syndiniales temporal dynamics***

306 By studying temporal patterns of Syndiniales across 3 time-series we highlighted a small number of

307 CCs that are recurrent over time, persistent through seasons and some indicators of parasite  
308 community variation. The recurrence of these taxa could be associated with rhythmic host patterns  
309 like annual blooms, as parasites can respond quickly to elevated host density [22, 26]. Taxa  
310 persistent throughout seasons could further indicate a generalist and opportunistic parasite behavior,  
311 infecting the hosts that are present during each season, while surviving in spore form during low host  
312 densities [23, 50]. Flexible host-parasite associations have already been described in coastal  
313 estuaries using co-occurrence networks [22]. Alternatively, parasites cannot persist below a critical  
314 host threshold [28], which questions the trophic mode of the detected persistent Syndiniales. Up to  
315 date only parasitic and parasitoid Syndiniales have been described [47]. Nevertheless, parasitism is  
316 a mode of symbiosis along a parasite-mutualist continuum and transitions from one mode to the  
317 other should not be excluded [51].

318

### 319 ***Syndiniales as potential indicators of ecosystem change ?***

320 Our analysis also highlighted Syndiniales CCs that were both recurrent over time and good indicators  
321 of parasite community abundance variation. These Syndiniales CC hold the potential for monitoring  
322 changes in environmental microbial communities, reflecting shifts not only among the Syndiniales  
323 communities but also mirroring their associated host community. The absence of these Syndiniales  
324 CC could, for instance, indicate a shift in microbial community composition during or after an  
325 environmental perturbation. For instance, in marine environments, multicellular parasites (e.g.  
326 trematodes) have been employed as bioindicators of host physiology in response to accumulating  
327 pollution for environmental monitoring [52]. The diversity of frog and fish endoparasites was shown  
328 to reflect their surrounding ecological conditions. Selecting endoparasite taxa that are sensitive to  
329 environmental perturbation is crucial for a potential bioindicator. In that respect, our analysis  
330 throughout a 6-10 years of abundance information and metadata suggest that dinoflagellate  
331 parasites could be used for marine habitat monitoring as it has been done with diatoms, ciliates and  
332 foraminifera [30]. Behind the blackbox of Syndiniales taxonomy could be hidden a promising global  
333 ecosystem change indicator; thanks to their worldwide distribution [14], abundance [22], quick  
334 response time to host community shifts (Anderson & Harvey 2020) and intimate implication in marine

335 food webs [26].

336

### 337 ***SSNs as integrative tools to prioritize unassigned protist taxa***

338 In this integrative study we have used a sequence similarity network to explore the ecology of the  
339 main components of the unassigned protist microbiome by combining 6 metabarcoding datasets.  
340 SSNs are relevant and efficient analytical tools for addressing the unassigned microbiome challenge  
341 as they allow studying simultaneously large datasets, in order to categorize and prioritize unassigned  
342 sequences. They have been recently employed among prokaryotes for surveying the coding part of  
343 genomes and metagenomes [6] and taxonomy across extreme aquatic environments [12]. By  
344 exploring the biogeography of these sequences we can reveal core taxa shared across ecosystems  
345 [12, 53]. Here we have explored both biogeographical and temporal patterns of protists at the species  
346 level without requiring a reference taxonomic match. Our FAIR (Findable, Accessible, Interoperable  
347 and Reusable) computational workflow that allows to integrate data from heterogeneous ecosystem  
348 sampling protocols, such as coastal time-series and open sea campaigns and can be applied to any  
349 targeted protist group of any metabarcoding dataset, of the same marker gene, for example  
350 originating from the metaPR2 database [54] and Ocean Barcode Atlas [55]. The taxa identified by  
351 the network could then be specifically targeted for *in situ* hybridisation [43] and isolation for single-  
352 cell omics [31]. Other approaches to reduce the unassigned taxonomic load encompass long-read  
353 sequencing [16], sequencing multiple metabarcoding markers [30] and combining metabarcoding  
354 and microscopy [34]. The unassigned microbiome holds an unexplored potential of novel taxa and  
355 functions that will surely challenge the current view of microbial ecology in the ocean and beyond [5,  
356 31, 56].

## 357 **Materials and Methods**

### 358 ***Gathering and homogenisation of metabarcoding datasets***

359 Metabarcoding datasets of 18S rDNA marker sequences containing the variable region V4 and  
360 originating from 6 distinct sampling projects were gathered. The datasets include three temporal  
361 series of bimensual samplings at a single station: ASTAN in Roscoff, English Channel, France (8

362 years of data), BBMO in Blanes Bay, Mediterranean Sea, Spain (10 years of data) and SOLA in  
363 Banyuls-sur-Mer, Mediterranean Sea, France (9 years of data) (Fig. S1D); two oceanographic  
364 campaigns of punctual samplings across 148 locations: Malaspina Expedition (122 stations,  
365 circumglobal Tropical/Subtropical Ocean) and MOOSE (26 stations, Mediterranean Sea) (Fig.  
366 S1B,C); and one European project of punctual samplings at 6 marine coastal stations: BioMarKs  
367 project (samples from: Oslo, Norway; Roscoff, France; Varna, Bulgaria; Gijon, Spain; Barcelona,  
368 Spain; Naples, Italy). Sequencing was done with Illumina MiSeq technology, except for the BioMarKs  
369 project sequenced by 454 pyrosequencing. Each metabarcoding dataset contained the abundance  
370 tables of reads clean-processed and inferred into ASVs (OTUs for BioMarKs) and their taxonomic  
371 affiliation (details in Table S1). The initial global dataset contained 539 546 metabarcodes. For  
372 homogenisation purposes, the same two filtering conditions were applied independently to each of  
373 the 6 datasets (Fig. S1A, Step 1): removal of sequences corresponding to metazoans, terrestrial  
374 plants (Streptophyta) and macroalgae (Florideophyceae, Bangiophyceae, Phaeophyceae, and  
375 Ulvophyceae); removal of sequences having less than 80% identity with reference databases. The  
376 latter threshold was chosen according to the original preprocessing of the datasets: the MOOSE  
377 dataset had beforehand implemented a minimum identity threshold of 80% and Malaspina and  
378 BBMO of 95%. A 95% filter was considered too stringent, as too many unknown sequences of  
379 interest might be removed, a 80% threshold was applied to the global dataset for homogenisation.  
380 The global abundance table resulting from the homogenisation workflow involved at this stage 343  
381 165 metabarcodes, and each sample was normalized by total read number and scaled from 0 to 1.  
382

383 To account for variations in the taxonomic assignment procedure (assignment tools, database  
384 versions) across datasets, a new taxonomic assignment (Fig. S1A, Step 2) was performed on the  
385 global set of metabarcodes with the PR2 database (version 4.12.0, released on 08.08.2019,  
386 <https://pr2-database.org> ; blast parameters: -evalue 0.01 -max\_target\_seqs 15, [57]). Only the best  
387 hit (best e-value) of each alignment was kept. These new assignments were filtered again for  
388 multicellular taxa and only sequences with a length greater to 200 bp were kept (Fig. S1A, Step 3).  
389 The PR2 database includes 8 taxonomic ranks: kingdom, supergroup, division, class, order, family,

390 genus, and species. To avoid prokaryotic contamination at the kingdom level, an assignment was  
391 performed using the SILVA database (<https://www.arb-silva.de/>, version 138) implemented in the  
392 DADA2 algorithm [58]. 3 874 prokaryotic metabarcodes were removed out of the 4 519 unassigned  
393 sequences at the kingdom level. The taxonomic ranks that were left unassigned were marked as  
394 “Unknown” and the taxonomy of the sequence was considered unassigned at this given rank.  
395 Unassigned ranks located between attributed ranks were regarded as gaps in the taxonomic  
396 hierarchy and not as unassigned ranks. The diversity and abundance of unassigned sequences were  
397 explored on Rstudio (R version 4.1.1, [59]), using the packages: ‘data.table’, ‘vegan’, ‘ggplot2’, ‘ggsci’  
398 and ‘gridExtra’.

399

#### 400 ***Homogenisation and analysis of environmental data***

401 Our global dataset included 1 531 samples (ASTAN: 374, BBMO: 327, SOLA: 154, Malaspina: 289,  
402 MOOSE: 272) (Table S1). The metadata and environmental information associated with the studied  
403 samples were retrieved from the initial studies [60-66] and supplemented with public oceanographic  
404 databases (cf. additional information in the next paragraph). The information contained 14 metadata  
405 variables: name of the campaign, sampled region, station (for oceanographic campaigns),  
406 sequencing technology, sampling date, year, month, season, depth (m), depth type (surface (depth  
407  $\leq 5$  m), deep maximum chlorophyll (DCM), mesopelagic zone (depth  $\geq 200$  m), bathypelagic zone  
408 (depth  $\geq 1\ 000$  m)), sampled size fraction, latitude, longitude). The 3 temporal series datasets  
409 (ASTAN, SOLA, BBMO) were sampled only at surface, BioMarKs dataset was sampled at surface  
410 and DCM, while the 2 oceanographic campaigns (MOOSE and Malaspina) were sampled at surface,  
411 DCM, mesopelagic and bathypelagic zones (up to 2 000 m depth for MOOSE and 4 000 m for  
412 Malaspina). The sampled size fractions are: 0-0.2  $\mu\text{m}$ , 0.2-3  $\mu\text{m}$ , 0.2-0.8  $\mu\text{m}$ , 0.8-3  $\mu\text{m}$ , 0.8-20  $\mu\text{m}$ ,  
413 3-20  $\mu\text{m}$ , 20-2 000  $\mu\text{m}$ . The information contained as well 10 environmental variables: temperature  
414 ( $^{\circ}\text{C}$ ), salinity (PSU), pH, concentrations of oxygen (ml/L), nitrate ( $\mu\text{mol/L}$ ), nitrite ( $\mu\text{mol/L}$ ), ammonium  
415 ( $\mu\text{mol/L}$ ), phosphate ( $\mu\text{mol/L}$ ), silicate ( $\mu\text{mol/L}$ ) and chlorophyll-*a* ( $\mu\text{g/L}$ ). For ASTAN and BioMarKs  
416 datasets, when *in situ* environmental variables were missing, metadata were retrieved from public  
417 oceanographic databases (SOMLIT database (<https://www.somlit.fr>) ; World Ocean Database



418 (<https://www.ncei.noaa.gov/access/world-ocean-database-select/dbsearch.html>), SeaDataNet  
419 (<https://cdi.seadatanet.org/search>)). No additional information could be retrieved for 2 locations  
420 (Varna and Gijon). The environmental data and metadata were explored on Rstudio (R version 4.1.1),  
421 using the packages: 'maps', 'tidyverse', 'sp', 'reshape2', 'tidyr', 'ade4', 'factoextra' (Principal  
422 Component Analysis), 'ggplot2', 'ggsci' and 'gridExtra'.

423

#### 424 ***Sequence Similarity Network as a framework for heterogeneous datasets comparison***

425 The 343,165 metabarcodes were aligned against each other with the following options: e-value <  
426 1e-4 ; >80% coverage for both subject and query (except for the alignments involving SOLA  
427 sequences (maximum sequence length = 230 bp compared to a mean of 430 bp for other datasets)  
428 in which case the coverage threshold was applied only to the SOLA sequence in order to avoid a  
429 misrepresentation of SOLA sequences in our analysis). Self-hits and reciprocal hits (same query-  
430 subject pair) were discarded.. The filtered blast output (2 942 982 alignments) was used to cluster  
431 sequences by similarity in a Sequence Similarity Network (SSN), with 'igraph' R package (version  
432 1.2.6, <https://igraph.org/r/>, [67]). The sequences (i.e., the network nodes) were labeled according to  
433 metadata and taxonomic affiliation. The sequences were clustered into Connected Components  
434 (CCs) by setting an identity threshold of 100% sequence similarity, and CCs involving less than 6  
435 sequences were removed (this number of 6 was chosen in order to enable the representativity of all  
436 6 datasets in small CCs. The taxonomic homogeneity of CCs in the network was evaluated for known  
437 sequences at the genus level, and if only a single genus assignment was found this name was  
438 extrapolated to the other nodes of the CC even if these ones were of unknown genera. Thus, CCs  
439 were considered here as a proxy for studying taxonomic diversity at the genus level. The final  
440 network was composed of 12 619 CCs.

441

#### 442 ***Spatio-temporal patterns of metabarcodes and CCs***

443 CCs including only Syndiniales sequences unassigned at genus level were extracted from the  
444 network (4 245 CCs; 33.6% of network and 47.6% of unassigned network CCs at genus level, Fig.  
445 S7A, Fig. S8). The distribution of clusters across marine environments and time was explored with

446 R functions that were coded to extract the sequence attributes related to sampling data in each CC  
447 (location, dataset, depth, season month). A Redundancy Analysis (RDA) was performed on the  
448 abundance matrix of Syndiniales CCs using the metadata for Tropical/Subtropical Ocean and  
449 Mediterranean sea samples as explanatory variables. ANOVA tests were run to assess the  
450 robustness of the global RDA (all environmental variables included) and of the first two dimensions  
451 of the RDA with selected environmental variables. Both the RDA and ANOVA were run via the *vegan*  
452 package. Potential Syndiniales host communities were compared with the Jaccard dissimilarity index  
453 of the based on the Bray-Curtis compositional dissimilarity of abundances [68]. Jaccard index was  
454 computed with the *vegdist* function of the 'vegan' package, according to the formula:  $2B/(1+B)$ , where  
455 B is Bray-Curtis dissimilarity. The temporal patterns of Syndiniales among each Time Series (ASTAN,  
456 BBMO, SOLA) were explored for both assigned and unassigned genera clusters (4 317 CCs ; 34.2%  
457 of network, Fig S7B). Diversity indexes (species richness (S), Shannon's diversity (H) and reverse  
458 Pielou index (J), using the *vegan* package) and statistical metrics (mean abundance per month) were  
459 computed. The Escoufier's equivalent vector method was applied on CCs present at least 5 times  
460 across each time series. This method was run with the package *pastecs* and sorted clusters  
461 according to their correlation to a principal component analysis (PCA) [69]. The cumulated  
462 correlation level chosen was 75% in order to avoid retrieving clusters with negligible correlation (100%  
463 would result in retrieving the whole dataset). The rhythmicity of CCs across time was computed by  
464 the Lomb-Scargle Periodogram (LSP) [70] via the *lomb* package. Each CC was associated with a  
465 PNmax value, a p-value and a rhythmicity period (in days). The LSP method was applied according  
466 to Lambert et al., 2019 and is particularly well suited for our time-series data, as it allows us to detect  
467 the periodic patterns in unevenly sampled data. The PNmax is the decision variable corresponding  
468 to the peak normalized power, and CCs were considered rhythmic for a  $PN_{max} > 10$  (i.e. p-value <  
469 0.01). Graphical representations were plotted on Rstudio (R version 4.1.1) and Python (v3.8,  
470 package 'seaborn').

471

## 472 **Acknowledgements**

473 This work was supported by the *Institut des Sciences du Calcul et des Données* (ISCD) of Sorbonne

474 University via funding from the project FORMAL (From ObseRving to Modeling oceAn Life,  
475 <https://iscd.sorbonne-universite.fr/research/sponsored-junior-teams/formal-2/>). The authors thank  
476 the researchers that provided the datasets and metadata for this work: N Simon and M Caracciolo  
477 (Ecology of Marine Plankton (ECOMAP), Station Biologique de Roscoff, France) for the ASTAN time  
478 series, M Mendez-Sandin (Systematic Biology, Dept. of Organismal Biology Uppsala University,  
479 Sweden) for the MOOSE campaign, R Logares (Institut de Ciències del Mar (ICM), Barcelona, Spain)  
480 for the Malaspina campaign, Blanes Bay Observatory (BBMO) time series and the BioMarKs project,  
481 P Galand (Laboratory of Microbial Oceanography, Banyuls-sur-Mer, France) for the SOLA time  
482 series. All analyses of this work were performed remotely on the AbiMs cluster of the marine station  
483 of Roscoff (<http://abims.sb-roscoff.fr>). L Bittner acknowledges the Institut Universitaire de France for  
484 her 5-year nomination as Junior Member (2020-2025). □

## 485 **Data accessibility**

486 Scripts, data and Rmarkdown files necessary to run all the analyses included in this work are  
487 publicly available on the github page [https://github.com/IrisRizos/Unassigned\\_Protists\\_SSN](https://github.com/IrisRizos/Unassigned_Protists_SSN).

488

## 489 **References**

- 490 1. Forster D, Bittner L, Karkar S, Dunthorn M, Romac S, Audic S, et al. Testing ecological  
491 theories with sequence similarity networks: marine ciliates exhibit similar geographic  
492 dispersal patterns as multicellular organisms. *BMC Biol.* 2015 ;13(1):16;  
493 <http://bmcbiol.biomedcentral.com/articles/10.1186/s12915-015-0125-5>.
- 494
- 495 2. Galperin MY, Koonin EV. From complete genome sequence to ‘complete’  
496 understanding? *Trends in Biotechnology.* 2010;28(8):398–  
497 406;<https://linkinghub.elsevier.com/retrieve/pii/S0167779910000892>.
- 498
- 499 3. Modha S, Robertson DL, Hughes J, Orton RJ. Quantifying and Cataloguing Unknown  
500 Sequences within Human Microbiomes. Arumugam M, editor. *mSystems.* 2022;7(2):e01468-

501 21; <https://journals.asm.org/doi/10.1128/msystems.01468-21>.

502

503 4. Wyman SK, Avila-Herrera A, Nayfach S, Pollard KS. A most wanted list of conserved  
504 microbial protein families with no known domains. Ouzounis CA, editor. PLoS ONE.  
505 2018;13(10):e0205749; <https://dx.plos.org/10.1371/journal.pone.0205749>.

506

507 5. Bernard G, Pathmanathan JS, Lannes R, Lopez P, Baptiste E. Microbial Dark Matter  
508 Investigations: How Microbial Studies Transform Biological Knowledge and Empirically  
509 Sketch a Logic of Scientific Discovery. Genome Biology and Evolution. 2018;10(3):707–15;  
510 <https://academic.oup.com/gbe/article/10/3/707/4840377>.

511

512 6. Vanni C, Schechter MS, Acinas SG, Barberán A, Buttigieg PL, Casamayor EO, et al.  
513 Unifying the known and unknown microbial coding sequence space. eLife. 2022;11:e67667;  
514 <https://elifesciences.org/articles/67667>.

515

516 7. Jaroszewski L, Li Z, Krishna SS, Bakolitsa C, Wooley J, Deacon AM, et al. Exploration  
517 of Uncharted Regions of the Protein Universe. Chothia C, editor. PLoS Biol.  
518 2009;7(9):e1000205; <https://dx.plos.org/10.1371/journal.pbio.1000205>.

519

520 8. Meng A, Corre E, Probert I, Gutierrez-Rodriguez A, Siano R, Annamale A, et al.  
521 Analysis of the genomic basis of functional diversity in dinoflagellates using a transcriptome-  
522 based sequence similarity network. Mol Ecol 2018;27(10):2365–80;  
523 <https://onlinelibrary.wiley.com/doi/10.1111/mec.14579>.

524

525 9. Meng A, Marchet C, Corre E, Peterlongo P, Alberti A, Da Silva C, et al. A de novo  
526 approach to disentangle partner identity and function in holobiont systems. Microbiome.  
527 2018;6(1):105; [https://microbiomejournal.biomedcentral.com/articles/10.1186/s40168-018-](https://microbiomejournal.biomedcentral.com/articles/10.1186/s40168-018-0481-9)  
528 0481-9.

529

530 10. Tara Oceans Coordinators, Carradec Q, Pelletier E, Da Silva C, Alberti A, Seeleuthner  
531 Y, et al. A global ocean atlas of eukaryotic genes. *Nat Commun.* 2018;9(1):373;  
532 <http://www.nature.com/articles/s41467-017-02342-1>.

533

534 11. Ramond P, Sourisseau M, Simon N, Romac S, Schmitt S, Rigaut-Jalabert F, et al.  
535 Coupling between taxonomic and functional diversity in protistan coastal communities:  
536 Functional diversity of marine protists. *Environ Microbiol.* 2019;21(2):730–49;  
537 <http://doi.wiley.com/10.1111/1462-2920.14537>.

538

539 12. Zamkovaya T, Foster JS, de Crécy-Lagard V, Conesa A. A network approach to  
540 elucidate and prioritize microbial dark matter in microbial communities. *ISME J.*  
541 2021;15(1):228–44; <https://www.nature.com/articles/s41396-020-00777-x>.

542

543 13. Sunagawa S, Coelho LP, Chaffron S, Kultima JR, Labadie K, Salazar G, et al.  
544 Structure and function of the global ocean microbiome. *Science.* 2015;348(6237):1261359–  
545 1261359; <https://www.sciencemag.org/lookup/doi/10.1126/science.1261359>.

546

547 14. de Vargas C, Audic S, Henry N, Decelle J, Mahe F, Logares R, et al. Eukaryotic  
548 plankton diversity in the sunlit ocean. *Science.* 2015;348(6237):1261605–1261605;  
549 <https://www.sciencemag.org/lookup/doi/10.1126/science.1261605>.

550

551 15. Strassert JFH, Karnkowska A, Hehenberger E, del Campo J, Kolisko M, Okamoto N,  
552 et al. Single cell genomics of uncultured marine alveolates shows paraphyly of basal  
553 dinoflagellates. *ISME J.* 2018;12(1):304–8; <http://www.nature.com/articles/ismej2017167>.

554

555 16. Burki F, Sandin MM, Jamy M. Diversity and ecology of protists revealed by  
556 metabarcoding. *Current Biology.* 2021;31(19):R1267–80;

557 <https://linkinghub.elsevier.com/retrieve/pii/S0960982221010563>.

558

559 17. Cai R, Kayal E, Alves-de-Souza C, Bigeard E, Corre E, Jeanthon C, et al. Cryptic  
560 species in the parasitic Amoeboophrya species complex revealed by a polyphasic approach.  
561 Sci Rep. 2020;10(1):2531;<http://www.nature.com/articles/s41598-020-59524-z>.

562

563 18. Singer D, Seppey CVW, Lentendu G, Dunthorn M, Bass D, Belbahri L, et al. Protist  
564 taxonomic and functional diversity in soil, freshwater and marine ecosystems. Environment  
565 International. 2021;146:106262;  
566 <https://linkinghub.elsevier.com/retrieve/pii/S0160412020322170>.

567

568 19. Guillou L, Viprey M, Chambouvet A, Welsh RM, Kirkham AR, Massana R, et al.  
569 Widespread occurrence and genetic diversity of marine parasitoids belonging to Syndiniales  
570 (Alveolata). Environmental Microbiology. 2008;10(12):3349–  
571 65;<https://onlinelibrary.wiley.com/doi/10.1111/j.1462-2920.2008.01731.x>.

572

573 20. Clarke LJ, Bestley S, Bissett A, Deagle BE. A globally distributed Syndiniales parasite  
574 dominates the Southern Ocean micro-eukaryote community near the sea-ice edge. ISME J.  
575 2019;13(3):734–7;<http://www.nature.com/articles/s41396-018-0306-7>.

576

577 21. Cleary AC, Durbin EG. Unexpected prevalence of parasite 18S rDNA sequences in  
578 winter among Antarctic marine protists. J Plankton Res. 2016;38(3):401–17;  
579 <https://academic.oup.com/plankt/article-lookup/doi/10.1093/plankt/fbw005>.

580

581 22. Anderson SR, Harvey EL. Temporal Variability and Ecological Interactions of Parasitic  
582 Marine Syndiniales in Coastal Protist Communities. Campbell BJ, editor. mSphere. 2020;5(3);  
583 <https://journals.asm.org/doi/10.1128/mSphere.00209-20>.

584

- 585 23. Käse L, Metfies K, Neuhaus S, Boersma M, Wiltshire KH, Kraberg AC. Host-parasitoid  
586 associations in marine planktonic time series: Can metabarcoding help reveal them? Amato  
587 A, editor. PLoS ONE. 2021;16(1):e0244817;  
588 <https://dx.plos.org/10.1371/journal.pone.0244817>.  
589
- 590 24. Jephcott TG, Alves-de-Souza C, Gleason FH, van Ogtrop FF, Sime-Ngando T, Karpov  
591 SA, et al. Ecological impacts of parasitic chytrids, syndiniales and perkinsids on populations  
592 of marine photosynthetic dinoflagellates. Fungal Ecology. 2016;  
593 <https://linkinghub.elsevier.com/retrieve/pii/S175450481500032X>.  
594
- 595 25. Siano R, Alves-de-Souza C, Foulon E, Bendif EM, Simon N, Guillou L, et al.  
596 Distribution and host diversity of Amoebophryidae parasites across oligotrophic waters of the  
597 Mediterranean Sea. Biogeosciences. 2011;8(2):267–78;  
598 <https://bg.copernicus.org/articles/8/267/2011/>.  
599
- 600 26. Moran MA, Ferrer-González FX, Fu H, Nowinski B, Olofsson M, Powers MA, et al.  
601 The Ocean's labile DOC supply chain. Limnology & Oceanography.  
602 2022;Ino.12053;<https://onlinelibrary.wiley.com/doi/10.1002/lno.12053>.  
603
- 604 27. Farhat S, Le P, Kayal E, Noel B, Bigeard E, Corre E, et al. Rapid protein evolution,  
605 organellar reductions, and invasive intronic elements in the marine aerobic parasite  
606 dinoflagellate Amoebophrya spp. BMC Biol. 2021;19(1):1;  
607 <https://bmcbiol.biomedcentral.com/articles/10.1186/s12915-020-00927-9>.  
608
- 609 28. Okamura B, Hartigan A, Naldoni J. Extensive Uncharted Biodiversity: The Parasite  
610 Dimension. Integrative and Comparative Biology. 2018;  
611 <https://academic.oup.com/icb/advance-article/doi/10.1093/icb/icy039/5026008>.  
612

- 613 29. Rohde K. Ecology and Biogeography, Future Perspectives: Example Marine  
614 Parasites. *Geoinfor Geostat: An Overview*. 2016;4(2); [http://www.scitechnol.com/peer-](http://www.scitechnol.com/peer-review/ecology-and-biogeography-future-perspectives-example-marine-parasites-wRny.php?article_id=4869)  
615 [review/ecology-and-biogeography-future-perspectives-example-marine-parasites-](http://www.scitechnol.com/peer-review/ecology-and-biogeography-future-perspectives-example-marine-parasites-wRny.php?article_id=4869)  
616 [wRny.php?article\\_id=4869](http://www.scitechnol.com/peer-review/ecology-and-biogeography-future-perspectives-example-marine-parasites-wRny.php?article_id=4869).
- 617
- 618 30. Pawlowski J, Audic S, Adl S, Bass D, Belbahri L, Berney C, et al. CBOL Protist  
619 Working Group: Barcoding Eukaryotic Richness beyond the Animal, Plant, and Fungal  
620 Kingdoms. *PLoS Biol.*  
621 2012;10(11):e1001419;<https://dx.plos.org/10.1371/journal.pbio.1001419>.
- 622
- 623 31. del Campo J, Sieracki ME, Molestina R, Keeling P, Massana R, Ruiz-Trillo I. The  
624 others: our biased perspective of eukaryotic genomes. *Trends in Ecology & Evolution*.  
625 2014;29(5):252–9; <https://linkinghub.elsevier.com/retrieve/pii/S0169534714000640>.
- 626
- 627 32. Sibbald SJ, Archibald JM. More protist genomes needed. *Nat Ecol Evol*.  
628 2017;1(5):0145; <http://www.nature.com/articles/s41559-017-0145>.
- 629
- 630 33. Egge E, Elferink S, Vaultot D, John U, Bratbak G, Larsen A, et al. An 18S V4 rRNA  
631 metabarcoding dataset of protist diversity in the Atlantic inflow to the Arctic Ocean, through  
632 the year and down to 1000 m depth. *Earth Syst Sci Data*. 2021;13(10):4913–28;  
633 <https://essd.copernicus.org/articles/13/4913/2021/>.
- 634
- 635 34. Mugnai F, Megléc E, Abbiati M, Bavestrello G, Bertasi F, Bo M, et al. Are well-studied  
636 marine biodiversity hotspots still blackspots for animal barcoding? *Global Ecology and*  
637 *Conservation*. 2021;32:e01909;  
638 <https://linkinghub.elsevier.com/retrieve/pii/S2351989421004595>.
- 639
- 640 35. Bittner L, Gobet A, Audic S, Romac S, Egge ES, Santini S, et al. Diversity patterns of



641 uncultured Haptophytes unravelled by pyrosequencing in Naples Bay. *Mol Ecol.*  
642 2013;22(1):87–101; <https://onlinelibrary.wiley.com/doi/10.1111/mec.12108>.

643

644 36. Malviya S, Scalco E, Audic S, Vincent F, Veluchamy A, Poulain J, et al. Insights into  
645 global diatom distribution and diversity in the world's ocean. *Proc Natl Acad Sci USA.*  
646 2016;113(11);<https://pnas.org/doi/full/10.1073/pnas.1509523113>.

647

648 37. Kochin BF, Bull JJ, Antia R. Parasite Evolution and Life History Theory. *PLoS Biol.*  
649 2010=;8(10):e1000524; <https://dx.plos.org/10.1371/journal.pbio.1000524>.

650

651 38. Sheath DJ, Dick JTA, Dickey JWE, Guo Z, Andreou D, Britton JR. Winning the arms  
652 race: host–parasite shared evolutionary history reduces infection risks in fish final hosts. *Biol*  
653 *Lett.* 2018;14(7):20180363; <https://royalsocietypublishing.org/doi/10.1098/rsbl.2018.0363>.

654 39. Blanco-Bercial L, Parsons R, Bolaños L, Johnson R, Giovannoni S, Curry R. The  
655 protist community mirrors seasonality and mesoscale hydrographic features in the  
656 oligotrophic Sargasso Sea. Preprints; 2022 (37);  
657 [https://www.authorea.com/users/453879/articles/551657-the-protist-community-mirrors-](https://www.authorea.com/users/453879/articles/551657-the-protist-community-mirrors-seasonality-and-mesoscale-hydrographic-features-in-the-oligotrophic-sargasso-sea?commit=ba32b47ec0dff4865eb448dd0b5dd27d5f8cd15)  
658 [seasonality-and-mesoscale-hydrographic-features-in-the-oligotrophic-sargasso-](https://www.authorea.com/users/453879/articles/551657-the-protist-community-mirrors-seasonality-and-mesoscale-hydrographic-features-in-the-oligotrophic-sargasso-sea?commit=ba32b47ec0dff4865eb448dd0b5dd27d5f8cd15)  
659 [sea?commit=ba32b47ec0dff4865eb448dd0b5dd27d5f8cd15](https://www.authorea.com/users/453879/articles/551657-the-protist-community-mirrors-seasonality-and-mesoscale-hydrographic-features-in-the-oligotrophic-sargasso-sea?commit=ba32b47ec0dff4865eb448dd0b5dd27d5f8cd15).

660

661 40. Mahé F, de Vargas C, Bass D, Czech L, Stamatakis A, Lara E, et al. Parasites  
662 dominate hyperdiverse soil protist communities in Neotropical rainforests. *Nat Ecol Evol.*  
663 2017;1(4):0091; <http://www.nature.com/articles/s41559-017-0091>.

664

665 41. Lepère C, Domaizon I, Debroas D. Unexpected Importance of Potential Parasites in  
666 the Composition of the Freshwater Small-Eukaryote Community. *Appl Environ Microbiol.*  
667 2008;74(10):2940–9; <https://journals.asm.org/doi/10.1128/AEM.01156-07>.

668

- 669 42. Chambouvet A, Gower DJ, Jirků M, Yabsley MJ, Davis AK, Leonard G, et al. Cryptic  
670 infection of a broad taxonomic and geographic diversity of tadpoles by Perkinsea protists.  
671 Proc Natl Acad Sci USA. 2015;112(34);<https://pnas.org/doi/full/10.1073/pnas.1500163112>.  
672
- 673 43. Chauvet M, Debroas D, Moné A, Dubuffet A, Lepère C. Temporal variations of  
674 Microsporidia diversity and discovery of new host–parasite interactions in a lake ecosystem.  
675 Environmental Microbiology. 2022;1462-2920.15950;  
676 <https://onlinelibrary.wiley.com/doi/10.1111/1462-2920.15950>.  
677
- 678 44. Stern RF, Horak A, Andrew RL, Coffroth MA, Andersen RA, Küpper FC, et al.  
679 Environmental Barcoding Reveals Massive Dinoflagellate Diversity in Marine Environments.  
680 Goldstien SJ, editor. PLoS ONE. 2010;5(11):e13991;  
681 <https://dx.plos.org/10.1371/journal.pone.0013991>.  
682
- 683 45. Stoeck T, Bass D, Nebel M, Christen R, Jones MDM, Breiner HW, et al. Multiple  
684 marker parallel tag environmental DNA sequencing reveals a highly complex eukaryotic  
685 community in marine anoxic water. Molecular Ecology. 2010;19:21–31;  
686 <http://doi.wiley.com/10.1111/j.1365-294X.2009.04480.x>.  
687
- 688 46. Decelle J, Martin P, Paborstava K, Pond DW, Tarling G, Mahé F, et al. Diversity,  
689 Ecology and Biogeochemistry of Cyst-Forming Acantharia (Radiolaria) in the Oceans. Stal  
690 LJ, editor. PLoS ONE. 2013;8(1):e53598; <https://dx.plos.org/10.1371/journal.pone.0053598>.  
691
- 692 47. Bjorbækmo MFM, Evenstad A, Røsæg LL, Krabberød AK, Logares R. The planktonic  
693 protist interactome: where do we stand after a century of research? ISME J 2020;14(2):544–  
694 59; <http://www.nature.com/articles/s41396-019-0542-5>.  
695
- 696 48. Dallas TA, Han BA, Nunn CL, Park AW, Stephens PR, Drake JM. Host traits

- 697 associated with species roles in parasite sharing networks. *Oikos*. 2019;128(1):23–32;  
698 <https://onlinelibrary.wiley.com/doi/10.1111/oik.05602>.
- 699
- 700 49. Lima-Mendez G, Faust K, Henry N, Decelle J, Colin S, Carcillo F, et al. Determinants  
701 of community structure in the global plankton interactome. *Science*.  
702 2015;348(6237):1262073;<https://www.science.org/doi/10.1126/science.1262073>.
- 703
- 704 50. Hayashi A, Crombie A, Lacey E, Richardson A, Vuong D, Piggott A, et al. *Aspergillus*  
705 *Sydowii* Marine Fungal Bloom in Australian Coastal Waters, Its Metabolites and Potential  
706 Impact on *Symbiodinium* Dinoflagellates. *Marine Drugs*. 2016;14(3):59;  
707 <http://www.mdpi.com/1660-3397/14/3/59>.
- 708
- 709 51. Drew GC, Stevens EJ, King KC. Microbial evolution and transitions along the  
710 parasite–mutualist continuum. *Nat Rev Microbiol*. 2021;19(10):623–38;  
711 <https://www.nature.com/articles/s41579-021-00550-7>.
- 712
- 713 52. Sures B, Nachev M, Selbach C, Marcogliese DJ. Parasite responses to pollution: what  
714 we know and where we go in ‘Environmental Parasitology.’ *Parasites Vectors*.  
715 2017;10(1):65;[http://parasitesandvectors.biomedcentral.com/articles/10.1186/s13071-017-](http://parasitesandvectors.biomedcentral.com/articles/10.1186/s13071-017-2001-3)  
716 [2001-3](http://parasitesandvectors.biomedcentral.com/articles/10.1186/s13071-017-2001-3).
- 717
- 718 53. Shade A, Handelsman J. Beyond the Venn diagram: the hunt for a core microbiome:  
719 The hunt for a core microbiome. *Environmental Microbiology*. 2012;14(1):4–  
720 12;<https://onlinelibrary.wiley.com/doi/10.1111/j.1462-2920.2011.02585.x>.
- 721
- 722 54. Vulot D, Sim CWH, Ong D, Teo B, Biwer C, Jamy M, et al. metaPR 2 : a database  
723 of eukaryotic 18S rRNAmetabarcodes with an emphasis on protists. *Molecular Ecology*  
724 *Resources*. 2022;1755-0998.13674; <https://onlinelibrary.wiley.com/doi/10.1111/1755->

725 0998.13674.

726

727 55. Vernet C, Henry N, Lecubin J, Vargas C, Hingamp P, Lescot M. The Ocean barcode  
728 atlas: A web service to explore the biodiversity and biogeography of marine organisms. *Mol*  
729 *Ecol Resour.* 2021;21(4):1347–58; [https://onlinelibrary.wiley.com/doi/10.1111/1755-](https://onlinelibrary.wiley.com/doi/10.1111/1755-0998.13322)  
730 0998.13322.

731

732 56. Chust G, Vogt M, Benedetti F, Nakov T, Villéger S, Aubert A, et al. Mare Incognitum:  
733 A Glimpse into Future Plankton Diversity and Ecology Research. *Front Mar Sci.* 2017;4;  
734 <http://journal.frontiersin.org/article/10.3389/fmars.2017.00068/full>.

735

736 57. Guillou L, Bachar D, Audic S, Bass D, Berney C, Bittner L, et al. The Protist Ribosomal  
737 Reference database (PR2): a catalog of unicellular eukaryote Small Sub-Unit rRNA  
738 sequences with curated taxonomy. *Nucleic Acids Research.* 2012;41(D1):D597–  
739 604; [http://academic.oup.com/nar/article/41/D1/D597/1064851/The-Protist-Ribosomal-](http://academic.oup.com/nar/article/41/D1/D597/1064851/The-Protist-Ribosomal-Reference-database-PR2-a)  
740 Reference-database-PR2-a.

741

742 58. Callahan BJ, McMurdie PJ, Holmes SP. Exact sequence variants should replace  
743 operational taxonomic units in marker-gene data analysis. *ISME J.* 2017;11(12):2639–  
744 43; <http://www.nature.com/articles/ismej2017119>.

745

746 59. RStudio Team (2020). RStudio: Integrated Development for R. RStudio, PBC, Boston,  
747 MA URL: <http://www.rstudio.com/>.

748

749 60. Caracciolo M, Rigaut J, Jalabert F, Romac S, Mahé F, Forsans S, Gac J, et al. Seasonal  
750 dynamics of marine protist communities in tidally mixed coastal waters. *Molecular Ecology.*  
751 2022;31(14):3761–83; <https://onlinelibrary.wiley.com/doi/10.1111/mec.16539>.

752

- 753 61. Giner CR, Balagué V, Krabberød AK, Ferrera I, Reñé A, Garcés E, et al. Quantifying  
754 long-term recurrence in planktonic microbial eukaryotes. *Mol Ecol.* 2019;28(5):923–35;  
755 <https://onlinelibrary.wiley.com/doi/10.1111/mec.14929>.  
756
- 757 62. Giner CR, Pernice MC, Balagué V, Duarte CM, Gasol JM, Logares R, et al. Marked  
758 changes in diversity and relative activity of picoeukaryotes with depth in the world ocean.  
759 *ISME J.* 2020;14(2):437–49; <http://www.nature.com/articles/s41396-019-0506-9>.  
760
- 761 63. Lambert S, Tragin M, Lozano JC, Ghiglione JF, Vaulot D, Bouget FY, et al. Rhythmicity  
762 of coastal marine picoeukaryotes, bacteria and archaea despite irregular environmental  
763 perturbations. *ISME J.* 2019;13(2):388–401; [http://www.nature.com/articles/s41396-018-](http://www.nature.com/articles/s41396-018-0281-z)  
764 [0281-z](http://www.nature.com/articles/s41396-018-0281-z).  
765
- 766 64. Logares R, Deutschmann IM, Junger PC, Giner CR, Krabberød AK, Schmidt TSB, et  
767 al. Disentangling the mechanisms shaping the surface ocean microbiota. *Microbiome.*  
768 2020;8(1):55; [https://microbiomejournal.biomedcentral.com/articles/10.1186/s40168-020-](https://microbiomejournal.biomedcentral.com/articles/10.1186/s40168-020-00827-8)  
769 [00827-8](https://microbiomejournal.biomedcentral.com/articles/10.1186/s40168-020-00827-8).  
770
- 771 65. Pernice MC, Giner CR, Logares R, Perera-Bel J, Acinas SG, Duarte CM, et al. Large  
772 variability of bathypelagic microbial eukaryotic communities across the world's oceans. *ISME*  
773 *J.* 2016;10(4):945–58; <http://www.nature.com/articles/ismej2015170>.  
774
- 775 66. Massana R, Gobet A, Audic S, Bass D, Bittner L, Boutte C, et al. Marine protist  
776 diversity in European coastal waters and sediments as revealed by high-throughput  
777 sequencing: Protist diversity in European coastal areas. *Environ Microbiol.*  
778 2015;17(10):4035–49; <http://doi.wiley.com/10.1111/1462-2920.12955>.  
779
- 780 67. Csardi G, Nepusz T. The igraph software package for complex network research.

781 InterJournal, complex systems. 2006 Jan 11;1695(5):1-9.

782

783 68. Bray JR, Curtis JT. An Ordination of the Upland Forest Communities of Southern  
784 Wisconsin. Ecological Monographs. 1957;27(4):325–49;  
785 <https://onlinelibrary.wiley.com/doi/10.2307/1942268>

786

787 69. Robert P, Escoufier Y. A Unifying Tool for Linear Multivariate Statistical Methods: The  
788 RV- Coefficient. Journal of the Royal Statistical Society. Series C (Applied Statistics),  
789 1976;25(3), 257–265; <https://doi.org/10.2307/2347233>.

790

791 70. Ruf T. The Lomb-Scargle Periodogram in Biological Rhythm Research: Analysis of  
792 Incomplete and Unequally Spaced Time-Series. Biological Rhythm Research.  
793 1999;30(2):178–201; <https://www.tandfonline.com/doi/full/10.1076/brhm.30.2.178.1422>.

794

795

## 796 **Figure Legends**

797 **Fig. 1:** Relative abundance and diversity of unassigned metabarcodes. (A) Relative abundance of  
798 unassigned metabarcodes at each taxonomic level from kingdom to species. Colors represent the 6  
799 studied datasets. The horizontal red dashed line marks 50% of the dataset in terms of relative  
800 abundance. (B) Shannon Weiner diversity index calculated at genus level within major protist  
801 divisions in each dataset. Only metabarcodes unassigned at genus level are selected. Colors  
802 indicate the protist divisions that represent >50% of unassigned metabarcodes at genus level in each  
803 dataset (Fig. S5). (C) Relative abundance of assigned and unassigned metabarcodes within the  
804 class Dinophyceae (left) and Syndiniales (right) found in each dataset. Colors indicate the taxonomic  
805 status (Assigned/Unassigned) of metabarcodes at genus level.

806

807

808 **Fig. 2:** Distribution range of Connected Components (CCs) among Syndiniales orders unassigned

809 at genus level. The relative number (%) of CCs (y axis) within each Syndiniales order (Dino-Group-  
810 I to V and Unknown, i.e. unassigned order) is represented according to their occurrence across the  
811 6 sea regions defined in our metadata (Fig. S2). The raw number of CCs is indicated above each  
812 bar. The 4 245 CCs containing only unassigned sequences at genus level within each order of  
813 Syndiniales were selected. As Syndiniales order Dino-Group-IV contained only assigned sequences  
814 (at genus level) it was not included in the plot. Results are grouped on the x axis by the number of  
815 sea regions (defined by the PCA, Fig. S2) across which a CC is found (N). The colors indicate sea  
816 regions (for N=1) and pairs of sea regions (for N=2). The combination of sea regions is not illustrated  
817 for N>3. For N=2, "Others" include pairs of regions representing < 3.5% of pairs within each order.  
818 (N.b. The number of sampled stations is variable between sea regions with a higher number of  
819 stations sampled in Subtropical ocean (122 stations) and Mediterranean sea (35 stations). The other  
820 4 sea regions are represented by samplings at a single station. Also Subtropical ocean and  
821 Mediterranean sea include samplings located between 200 m and 4000 m deep. North sea and  
822 Black sea samples are from surface, DCM and anoxic layers. The English Channel and Bay of Biscay  
823 include only surface samples (Table S1).)

824

825 **Fig. 3:** Similarity in Syndiniales genera communities between Mediterranean sea and Subtropical  
826 ocean. (A) Proportion of Syndiniales CCs unassigned at genus level and shared between the  
827 Mediterranean sea (y axis) and the Subtropical ocean (x axis) per depth layer (SRF for surface, DCM  
828 for Deep Chlorophyll Maximum, MESO for mesopelagic layer (>200-1 000m), BATHY for  
829 bathypelagic layer (>1 000-4 000m)). The percentages illustrate major trends and not proportions  
830 (i.e. sums of percentages exceed 100% as combinations of shared CCs are not exclusive and some  
831 CCs are present in multiple depth layers). The number of samples from each depth layer for the  
832 Mediterranean sea are: SRF=571, DCM=88, MESO=97 and BATHY=46 and for the Subtropical  
833 ocean: SRF=136, DCM=13, MESO=30 and BATHY=110. The number of CCs found in each depth  
834 layer is: SRF=1 620, DCM=1 221, MESO=449 and BATHY=518 for the Mediterranean sea and  
835 SRF=1 726, DCM=943, MESO=611 and BATHY=1 281 for the Subtropical ocean. (B) Redundancy  
836 Analysis (RDA) for Mediterranean Sea and Subtropical Ocean data. The variation of abundance in  
837 unassigned Syndiniales CCs (black stars) is correlated to the variation of physicochemical

838 parameters (green arrows). The most pertinent environmental parameters allowing to differentiate  
839 the studied marine regions were selected (cf. Materials and Methods: Spatiotemporal patterns of  
840 metabarcodes and CCs). The samples are represented by different colors for Mediterranean Sea  
841 (orange) and Subtropical Ocean (blue). The shapes indicate the depth layer: dot; SRF, triangle; DCM,  
842 square; MESO, cross; BATHY and square/cross; NET (vertical profile samples (0-500m)). The  
843 dimensions of the input abundance matrix are: 4 037 CCs and 1 055 samples (768 samples for the  
844 Mediterranean Sea and 287 for the Subtropical Ocean). The global RDA (cf. Materials and Methods:  
845 Spatiotemporal patterns of metabarcodes and CCs) was statistically significant at 0.005% and the  
846 first 2 axes of the RDA with the selected explanatory variables (shown below) were significant at  
847 0.01%.

848

849 **Fig. 4:** Annual seasonal prevalence and abundance of rhythmic indicator Syndiniales CCs. The  
850 occurrence of CCs selected by the Escouffier's equivalent vectors and Lomb-Scargle Periodogram  
851 methods was studied across each time-series: (A) ASTAN; (B) BBMO; (C) SOLA. Relative  
852 abundance was computed per year as an average value of each month and is represented by square  
853 size. Colors indicate the seasonal prevalence of the CC throughout each year and the color gradient  
854 indicates the prevalence extent (i.e. 1 season prevalence indicated by the lightest color and 4  
855 seasons indicated by the darkest color of the gradient). A CC is considered prevalent if it is present  
856 at least once during each season. Taxonomically unassigned CCs at genus level are indicated by  
857 "unknown" in the CC ids (y axis).

858

859

860

861

862

863

864



865

866

867

868

869

870

871

872

873

874

875

876

877

878

# Graphical Abstract

bioRxiv preprint doi: <https://doi.org/10.1101/2022.07.24.501282>; this version posted July 24, 2022. The copyright holder for this preprint (which was not certified by peer review) is the author/funder, who has granted bioRxiv a license to display the preprint in perpetuity. It is made available under a [CC-BY-NC-ND 4.0 International license](#).

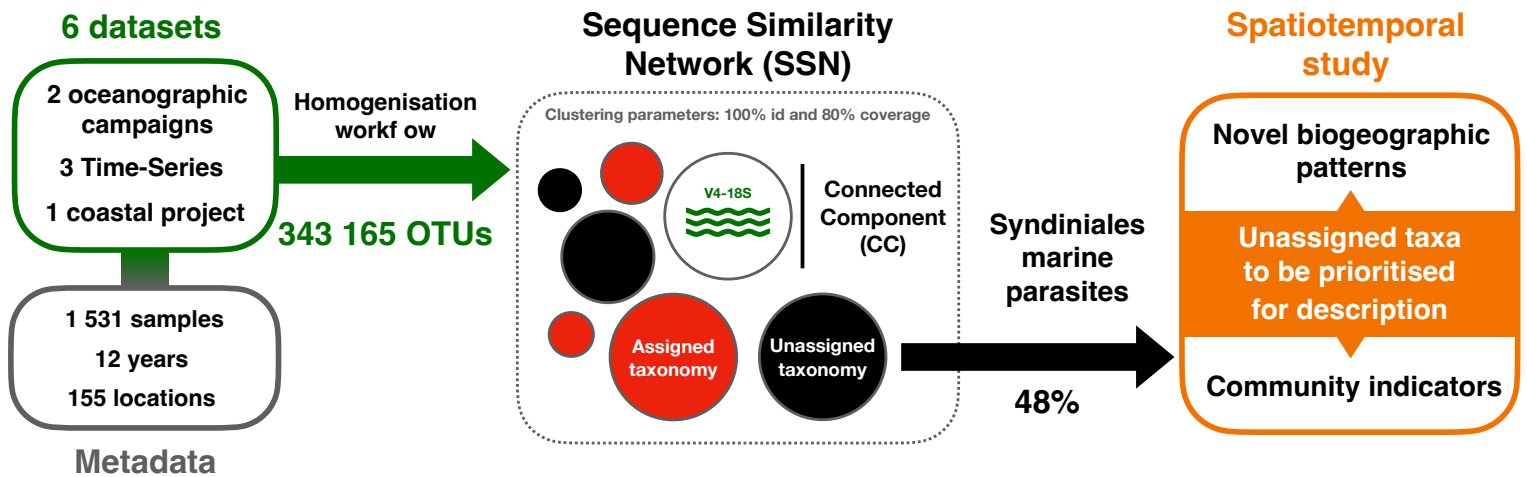


**Figure 1**

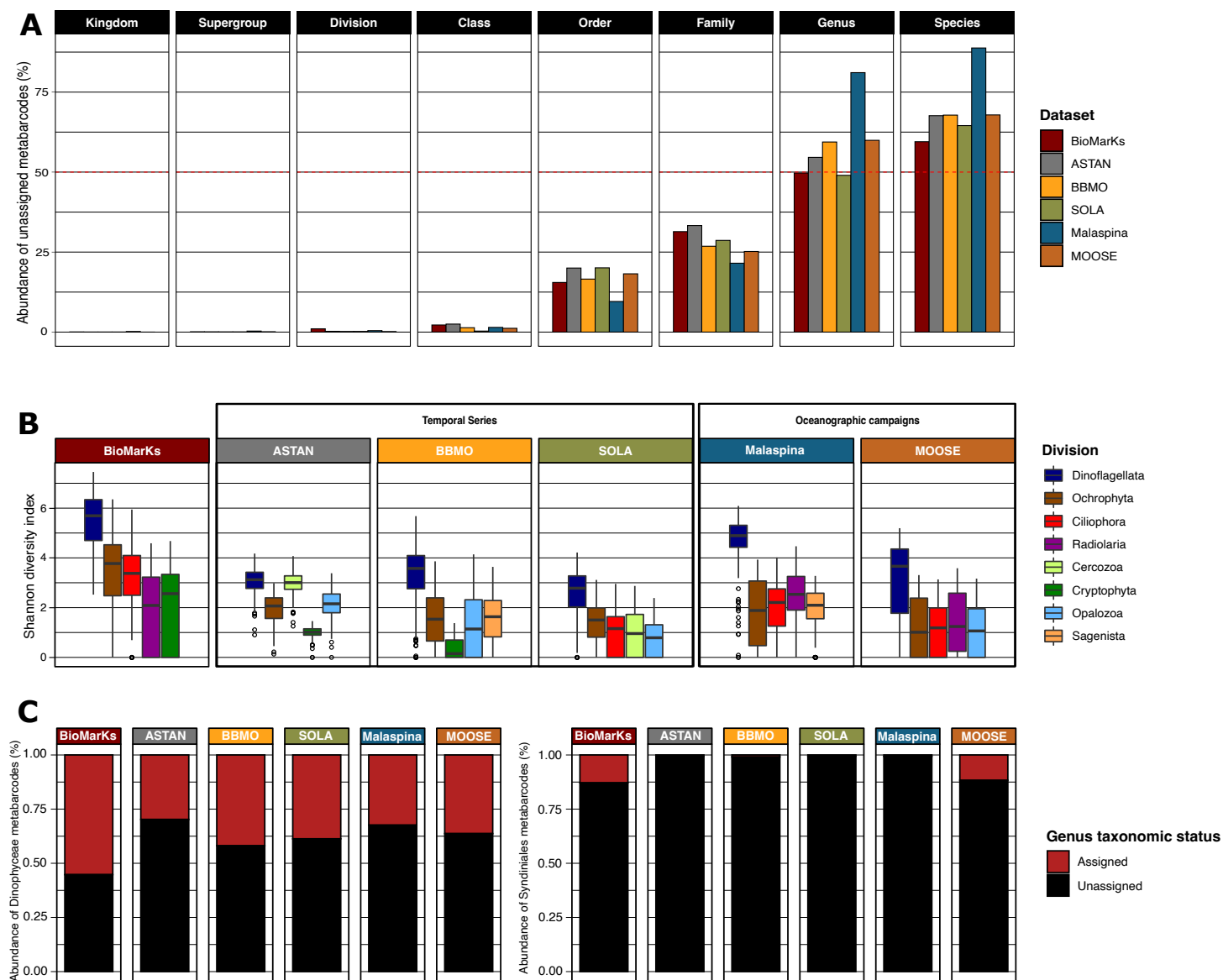


## Figure 2

bioRxiv preprint doi: <https://doi.org/10.1101/2022.07.24.501282>; this version posted July 24, 2022. The copyright holder for this preprint (which was not certified by peer review) is the author/funder, who has granted bioRxiv a license to display the preprint in perpetuity. It is made available under a [CC-BY-NC-ND 4.0 International license](#).

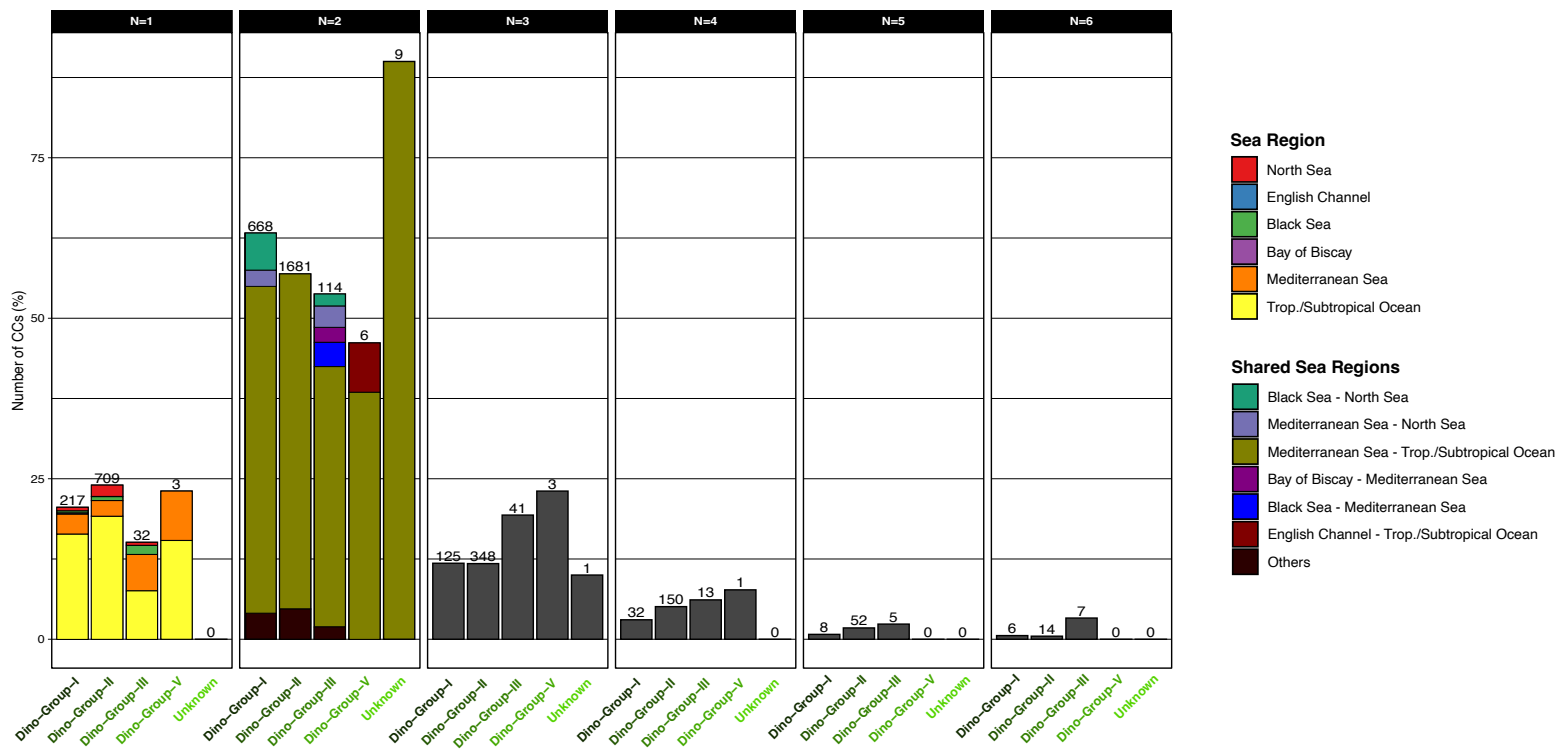


Figure 3

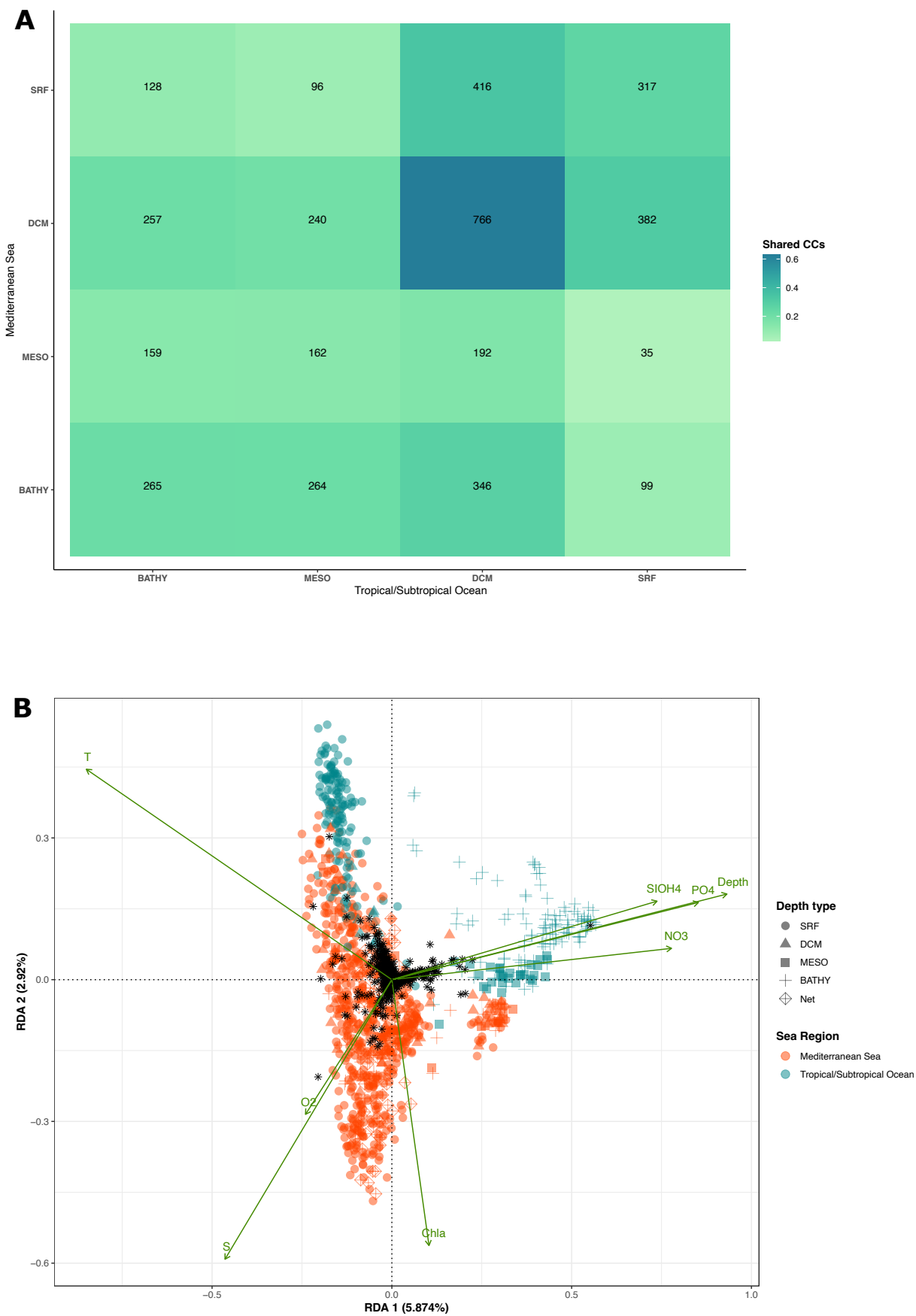
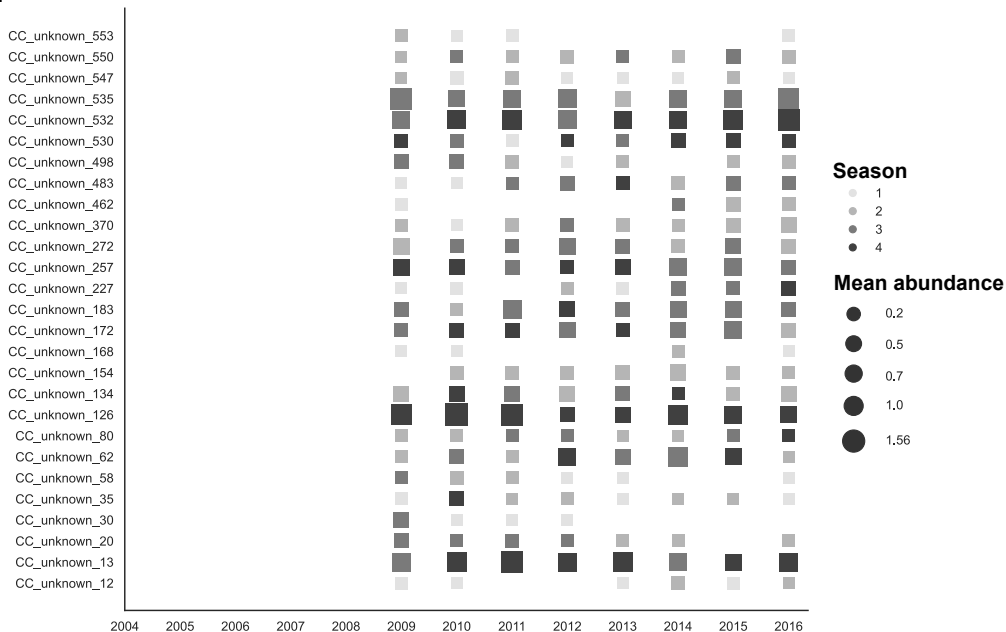


Figure 4

### A.ASTAN



### B.BBMO



### C.SOLA

